UC Berkeley
UC Berkeley Previously Published Works

Title
C–C Cleavage Approach to C–H Functionalization of Saturated Aza-Cycles

Permalink

Journal

ISSN

Authors
Roque, Jose B
Kuroda, Yusuke
Jurczyk, Justin
et al.

Publication Date

DOI

Peer reviewed

C—C Cleavage Approach to C—H Functionalization of Saturated Aza-Cycles

Jose B. Roque,
Department of Chemistry, University of California, Berkeley, Berkeley, California 94720, United States

Yusuke Kuroda,
Department of Chemistry, University of California, Berkeley, Berkeley, California 94720, United States

Justin Jurczyk,
Department of Chemistry, University of California, Berkeley, Berkeley, California 94720, United States

Li-Ping Xu,
Cherry L. Emerson Center for Scientific Computation, and Department of Chemistry, Emory University, Atlanta, Georgia 30322, United States

Jin Su Ham,
Department of Chemistry, University of California, Berkeley, Berkeley, California 94720, United States

Lucas T. Göttemann,
Department of Chemistry, University of California, Berkeley, Berkeley, California 94720, United States

Charis A. Roberts,
Department of Chemistry, University of California, Berkeley, Berkeley, California 94720, United States

Donovon Adpressa,
Structure Elucidation Group, Department of Analytical Research & Development, Merck & Company Inc., Boston, Massachusetts 02115, United States

Josep Saurí,
Structure Elucidation Group, Department of Analytical Research & Development, Merck & Company Inc., Boston, Massachusetts 02115, United States

Corresponding Authors Djamaladdin G. Musaev – dmusaev@emory.edu; **Charles S. Yeung** – charles.yeung@merck.com; **Richmond Sarpong** – rsarpong@berkeley.edu.

Leo A. Joyce,

Department of Process Research & Development, Merck & Company Inc., Rahway, New Jersey 07065, United States

Djamaladdin G. Musaev,

Cherry L. Emerson Center for Scientific Computation, and Department of Chemistry, Emory University, Atlanta, Georgia 30322, United States

Charles S. Yeung,

Disruptive Chemistry Fellow, Department of Discovery Chemistry, Merck & Company Inc., Boston, Massachusetts 02115, United States

Richmond Sarpong

Department of Chemistry, University of California, Berkeley, Berkeley, California 94720, United States

Abstract

Saturated cyclic amines (aza-cycles) are ubiquitous structural motifs found in pharmaceuticals, agrochemicals, and bioactive natural products. Given their importance, methods that directly functionalize aza-cycles are in high demand. Herein, we disclose a fundamentally different approach to functionalizing cyclic amines which relies on C—C cleavage and attendant cross-coupling. The initial functionalization step is the generation of underexplored N-fused bicyclo α-hydroxy-β-lactams under mild, visible light conditions using a Norrish–Yang process to affect α-functionalization of saturated cyclic amines. This approach is complementary to previous methods for the C—H functionalization of aza-cycles and provides unique access to various cross-coupling adducts. In the course of these studies, we have also uncovered an orthogonal, base-promoted opening of the N-fused bicyclo α-hydroxy-β-lactams. Computational studies have provided insight into the origin of the complementary C—C cleavage processes.

Graphical Abstract
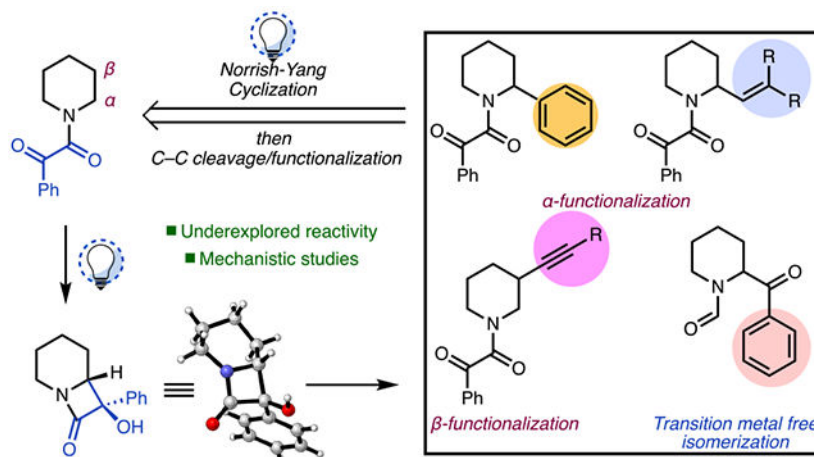
Keywords

cyclic amines; C—C cleavage; palladium; strain release; Norrish–Yang; cross-coupling

INTRODUCTION

Over the last two decades, the emergence of powerful and selective C—H functionalization methods has redefined approaches for synthesizing complex molecules and fine chemicals.[1] Recently, advances in site- and stereo-selective C(sp^3)—H functionalization have revolutionized the practice of late-stage functionalization (LSF) in the pharmaceutical, agrochemical, and materials industries, where there is strong motivation to identify architecturally complex sp^3-rich scaf-folds.[2] Among the many bioactive and privileged sp^3-rich scaffolds, piperidines are perhaps the most prevalent.[3,4] As such, synthetic methods for diversifying the piperidine framework are highly coveted. The state-of-the-art techniques that have been developed for this purpose employ directing groups on the piperidine nitrogen and require a highly specific and often harsh set of conditions that can be incompatible with functional groups on complex structures (Figure 1).[5,6] For example, Coldham showed that lithiation of *N*-Boc piperidine using Beak/Gawley-inspired conditions,[7] followed by transmetalation to an organozinc, set the stage for a Negishi-type cross-coupling (Figure 1a), building on the pyrrolidine arylation precedent of Campos and co-workers.[8] Knochel and co-workers later expanded on this work and demonstrated diastereoselective arylations of substituted piperidines,[9] as well as an example of *β*-functionalization. In this context, Baudoin and co-workers extended and generalized *β*-functionalization of *N*-Boc piperidines through ligand control.[10]

Recently, Seidel and co-workers developed an alternative one-pot protecting group-free approach to access *α*-functionalized cyclic amines,[11] albeit requiring strongly basic conditions. Alternatively, Sames and co-workers have reported one example of *α*-arylation with piperidines bearing an amidine directing group (see Figure 1b), using Ru catalysis and boronate esters, albeit in low yield.[12] Similarly, Maes and co-workers reported that pyridyl directing groups could affect the *α*-ruthenation of piperidines to yield arylated products; however, competing mono- and bis-arylation was observed.[13] In an exciting recent development, Yu and co-workers, Glorius and co-workers, and Gong and co-workers have shown that thioamide derivatives (Figure 1b) now enable enantioselective *α*-functionalization of a range of saturated aza-heterocycles including piperidines.[14-16] Other strategies have relied on photoredox catalysis,[17-19] intramolecular hydride transfer,[20] and C—H insertions via metal carbenoids.[21]

In the context of the cross-coupling step, the use of organozinc nucleophiles, in particular (i.e., Figure 1a), is highly attractive because it reduces to practice the *α*-arylation of piperidines to a standard cross-coupling reaction (i.e., the Negishi cross-coupling) under well-established and easily optimizable conditions using well-defined palladium complexes. In principle, in addition to *α*-zincated piperidyl nucleophiles, other main-group metal derivatives (e.g., from Li, Mg, B, Sn, etc.) would serve an analogous purpose. However, given the handling challenges associated with *α*-zinc-, *α*-lithio-, *α*-boryl-, and *α*-stannyl-derived piperidines,[22] we sought an alternative but easy-to-use and reliable strategy to generate a nucleophile at the *α*-position of the piperidine framework that would be stable in aerobic and aqueous environments, stored indefinitely, accessible in the enantiopure form, and deployed as required.

In this work, we report the utility of N-fused bicyclo α-hydroxy-β-lactams (e.g., **2,** Figure 1c), which are generated under mild, visible light ($\lambda = 400$–450 nm) conditions from phenyl keto amides (e.g., **1**),[23,24] as masked nucleophiles for the α-functionalization of piperidines and other saturated aza-cycles. Importantly, using the same α-hydroxy-β-lactam derivative of a saturated cyclic amine, arylation, vinylation, and alkynylation can be easily achieved using mild conditions. This work addresses a key gap in late-stage diversification via C—H functionalization/cross-coupling using a non-obvious C—C bond cleavage of a corresponding strained α-hydroxy-β-lactam. The work described herein represents the first example of using α-hydroxy-β-lactams to achieve α-functionalization via C—C bond cleavage, and importantly, it is the first demonstration of strain-initiated C—C cleavage and arylation at room temperature, attesting to the mildness of this approach to aza-cycle functionalization. Moreover, preliminary results toward β-functionalization of cyclic amines and a transition metal-free α-acylation are reported. The results described herein showcase the potential of the underexplored reactivity of α-hydroxy-β-lactams.

RESULTS AND DISCUSSION

Synthesis of α-Hydroxy-β-lactam Piperidine Derivative 2.

We commenced our studies by optimizing the protocol developed by Aoyama and co-workers[23] for the synthesis of α-hydroxy-β-lactam **2** (i.e., (±)-7-hydroxy-7-phenyl-1-azabicyclo[4.2.0]octan-8-one) from keto amide **1** (see Figure 2a). Ultimately, we found that irradiating **1** in the solid state with blue LEDs provided bicyclic N-fused bicyclo[4.2.0] β-lactam **2** in 66% isolated yield (70% NMR yield using Ph_3CH as the internal standard). Notably, this reaction can be perfomed on the gram scale (see the Supporting Information for details). Importantly, the same approach could easily be applied to related saturated nitrogen heterocycles (e.g., morpholine, azepane, azocane, etc.) and hence represents a programmable strategy for functionalizing these types of structural motifs (vide infra).

Optimization of the C—C Cleavage/Cross-Coupling.

With bicyclic hydroxylactam **2** in hand, we sought to identify conditions for its cross-coupling with bromobenzene on the basis of the precedent of Uemura.[25] We first set out to optimize the cross coupling conditions for α-arylation. A four-step mechanism (see Figure 2) is envisioned for the cross-coupling process, consistent with the proposal by Uemura.[25] This mechanistic scenario includes: (1) oxidative addition of Pd(0) to the aryl halide, (2) coordination/deprotonation of the tertiary hydroxy group, (3) β-C—C cleavage to liberate an α-palladated piperidine, and (4) reductive elimination of the Pd(II) species to regenerate the active Pd(0) catalyst and furnish the desired α-arylated product. Although strained ring systems such as *tert*-cyclobutanols have been employed previously in cross-coupling reactions,[26-28] there are no known examples using α-hydroxy-β-lactams, which introduce additional challenges such as control of their regioselective opening and the presence of other possible coordination sites.

After extensive optimization, we were successful in obtaining productive, regioselective, C—C cleavage/arylation at 40 °C (Table 1, entry 1). Importantly, the RuPhos ligand appeared to be uniquely effective in favoring the desired regioselective lactam ring opening

toward (or "proximal") the ring over the alternative, competing "distal" opening away from the ring and toward the carbonyl group of the β-lactam unit (see Figure 2 and Table 1, **3a$_d$**). The use of related Buchwald biaryl phosphine ligands led to diminished yields and selectivities. For example, the use of DavePhos or SPhos as supporting ligands produced the desired α-arylated piperidine in 48 and 18% NMR yields, respectively (entries 2–3). Cs_2CO_3 was identified as the optimal base, while other bases led to lower yields (entries 4–5). The choice of the solvent was critical, as only trace amounts of the desired α-arylated piperidine were obtained when 1,4-dioxane was used in place of toluene (entry 6). When the reaction was carried out at room temperature, only a 7% percent NMR yield of the target compound was observed with the rest of the material accounted for by the recovered starting material (entry 7). Contemporaneous with this effort, we leveraged a parallel data-rich experimentation approach to optimize this cross-coupling, which primarily relied on exploiting the aforementioned ligand effects. We recognized that faster initiation to a Pd(0) complex and a well-defined ligand-to-metal ratio may be beneficial to improving selectivity. [29,30] Indeed, by employing the commercially available KitAlysis technology [31] that features the latest G3/G4 palladium precatalysts of Buchwald's biaryl phosphine ligands, we quickly validated the unique effectiveness of RuPhos as a supporting ligand. The yields realized in this HTE screen were comparable to those obtained in the batch experiments (see the Supporting Information for details). However, by conducting the cross-coupling at room temperature using RuPhos-Pd-G4, we obtained a yield of 66% (Table 1, entry 8) for the desired adduct, a significant improvement over the previous yield of 7%. Raising the temperature to 40 °C, optimal conditions (entry 9) that were suitable across a wide range of substrates were identified.

Substrate Scope.

With the optimized conditions in hand and using **2** as a synthetic equivalent of an α-metalated piperidine, the scope of aryl halides in the cross-coupling was explored. Iodobenzene emerged as a superior coupling partner (69% isolated yield), outperforming bromobenzene under the established conditions to yield an α-phenyl piperidine product. While early attempts using phenyl triflate as a cross-coupling partner employing $Pd_2(dba)_3 \cdot CHCl_3$ and RuPhos as ligands led to complex mixtures, with RuPhos-Pd-G4, **3a** was obtained in 77% yield. Under modified conditions, aryl chlorides could also be used as electrophilic partners, albeit requiring a modification to XPhos as the optimal ligand and elevated temperatures. For instance, using chlorobenzene, α-phenyl piperidine **3a** was obtained in 33% yield, along with **3a$_D$** in 32% yield. Despite the diminished yields, aryl chlorides continue to be attractive cross-coupling partners because of their lower cost and abundance.[32] The α-arylation approach we have developed tolerates varying electronic influences on the aromatic halide. For example, electron-rich aryl halides perform well, providing the desired arylated products in good yield (**3a**–**3d**). Ethers and tertiary amine functional groups likewise do not adversely affect the yield of the cross-coupling (see **3c** and **3d**).

Electron-deficient coupling partners bearing substituents such as fluorine and chlorine efficiently couple as well (see **3e** and **3f**). Using the optimized conditions, site-selective coupling (aryl bromide vs aryl chloride) can be achieved on multiply halogenated substrates

(see **3f**), and the intact $C(sp^2)$–Cl bond in the resulting adduct can be employed as a functional handle for further functionalization.[32] Functional groups such as aldehydes and nitriles were also well accommodated using this method (see **3g, 3h**). Importantly, substituents at the *ortho* position of the aryl halide did not adversely hinder the reaction, and **3i** was obtained in 49% yield under our established cross-coupling conditions. An aryl bromide bearing a trifluoromethyl group at the *meta* position also led to the desired *α*-arylated product (**3j**) in modest yields. Heteroaromatics were also viable cross-coupling electrophiles, leading, for example, to indole **3k** and quinoline **3l** in 70 and 60% yields, respectively. As indicated above, improved yields were obtained using the precatalyst instead of the mix of $Pd_2(dba)_3 \cdot CHCl_3$ with RuPhos (see Table 1, entry 8 for conditions).

In Figure 3, products **3a, 3d, 3f, 3g, 3h, 3i**, and **3j** were isolated in higher yields under these conditions (see values in parenthesis and/or in maroon). Next, several other saturated heterocycles were examined in our programmed lactamization/arylation protocol. Pharmaceutically and agrochemically privileged scaffolds, such as morpholine, can be effectively functionalized through the aforementioned photochemical cyclization and importantly undergo C—C cleavage/cross-coupling to arrive at *α*-functionalized derivatives. For example, **4a** was obtained in 47% yield. Saturated heterocycles of varying ring sizes were also competent substrates. For example, azepane **4b** and azocane **4c** underwent *α*-arylation in 76 and 70% yields, respectively. Functional groups on the aza-cycle backbone, such as aryl (**4d**) and carbamates (**4e**), were also tolerated. The cis relationship between the phenyl and para substituent in the abovementioned examples is supported by 2D NMR (see the Supporting Information for details). The observed stereochemistry is dependent on the stereochemistry of the starting lactam, which participates in a stereospecific cross-coupling (*vide infra*). 3-substituted piperidines result in mixtures, and we are currently exploring conditions that may achieve selective lactamizations.

Given the complementarity of our approach to existing methods that arrive at *α*-metalated piperidines, we speculated that bicyclic hydroxylactam **2** could also be used to achieve additional *α*-functionalizations that are not readily realized using the previously established methodologies (Scheme 1).[7-18] Vinylation was readily achieved by employing the optimized conditions for arylation. For example, cross-coupling of *α*-hydroxy-*β*-lactam **2** with 1-bromo-2-methylprop-1-ene under the cross-coupling conditions led to vinylated intermediate **5** which underwent spontaneous cyclization to provide indolizidinone **6** in 30% yield. Next, we turned our attention to alkynylation. Surprisingly, when (bromoethynyl)triisopropylsilane was used as a coupling partner, **7** was obtained in 53% yield providing an avenue to *β*-alkynylation. Alkyne **7** presumably arises from *β*-hydride elimination of an *α*-palladated intermediate followed by re-insertion to generate the *β*-functionalized product (see Figure 4).[9,10] This example constitutes the first *β*-alkynylation of cyclic amines. Extension of the method to larger ring systems such as azepane (**8**) provided the desired *α*-alkynylated coupling product along with enamide **9a**, which supports the presumed *β*-hydride elimination of the initially generated alkyl palladium intermediate (Figure 4).[33,34] It is worth noting that the conditions for the alkynylation and vinylation cross-couplings have not been optimized. Furthermore, the C—C cleavage/cross-coupling is substrate-controlled as evidenced by the difference in the reaction outcome in switching from aryl halide to alkynyl

halide coupling partners. This example contrasts with the work of Baudoin and co-workers on piperidine derivatives,[10] where selectivity is achieved by means of the ligand control. Moreover, inspired by our observations in the alkynylation process (Scheme 1b) and, importantly, those of Knochel[9] and Baudoin,[10] we sought to identify opportunities for β-arylation of the saturated azacycles. Although Baudoin's studies required proper choice of the ligand to promote the β-H elimination/re-insertion sequence, using RuPhos as a starting point, we have found that heterocyclic halide **10** affords a 1:1 mixture of α-and β-functionalized cross-coupling adducts, pointing to a contributing effect of the cross-coupling electrophile partner to the observed selectivity (Figure 4). Further studies are ongoing to understand the factors that lead to β-functionalization and to developing a general ligand-controlled method. Thus, α-hydroxy-β-lactam **2** may be applied broadly with various cross-coupling partners.

The functionalization protocol reported here bears several key distinctions from the existing state-of-the-art approaches. First, we have demonstrated that mild conditions can be utilized to achieve the cross-coupling of aryl halides. This includes the coupling of **2** to aryl bromide **12** in 53% yield (Figure 5a), which contains a sensitive trifluoromethyldiazirine that is unstable to other conditions for α-functionalization such as photoredox conditions. By separating the photomediated functionalization from the cross-coupling, we have now overcome the challenge of cross-coupling photochemically sensitive groups such as the trifluoromethyldiazirine functional group which has been used in photoaffinity-triggered protein labeling.[35] Second, estrogen derivative **14** was readily functionalized with α-hydroxy-β-lactam **2** using the optimized precatalyst conditions, showcasing the potential for LSF of complex molecules (Figure 5b). Third, given the recent advances in leveraging Pd(II) oxidative addition complexes in cross-coupling reactions,[36] we demonstrated that complex **16** served as a stoichiometric coupling partner to afford desired product **17** in 20% yield (Figure 5c). Analogous to other cross-couplings, where low loadings of a metal precatalyst with precursor triflates or bromides that bear many coordinating functional groups are extremely challenging and low-yielding, stoichiometric organometallic cross-coupling partner **16** overcomes this challenge.[36] Fourth, when enantioenriched lactam **2** was subjected to the optimized cross-coupling conditions (Figure 5d), α-arylated piperidine **3a** was obtained with no appreciable erosion of enantiomeric excess, pointing to high fidelity in the stereospecific cross-coupling. Importantly, because our α-hydroxy-β-lactams are isolable and stable until deployed, this sequence of reactions allows us to broadly diversify aza-cycles with control of stereochemistry, thus achieving a "chiral, enantioenriched, organometallic equivalent" of α-metalated aza-cycles. On the basis of the absolute configuration of both hydroxylactam **2** and product **3a**, the overall coupling proceeds in a stereoretentive manner. This suggests that our reaction involves an intermediate step in which the C—C scission occurs with attendant stereoretentive palladation (see Figure 2b). Finally, the desired arylated product can be obtained in a one-pot process from ketoamide **1** by performing the Norrish–Yang reaction followed by palladium-catalyzed cross-coupling without isolating β-lactam **2** (Figure 5e). Future studies will seek to optimize the one-step protocol. It is worth noting that the keto amide group can be easily removed by treatment with NaOH (4 equiv) in THF/MeOH (Figure 5f) and no chromatographic purification step is required (see the Supporting Information for details).

Discovery of a Base-Promoted Rearrangement.

During the optimization process for the cross-coupling reported here, a rearranged product (**18**) resulting from cleavage of the distal bond of the β-lactam was isolated (see Table 2). Control experiments showed that this process occurs in the presence of Cs_2CO_3 without the need for a transition metal complex (Table 2, entry 1). Evaluation of a range of solvents led to the identification of toluene as a superior solvent for obtaining the highest yields (Table 2, entry 2). The formation of **18** from **2** did not proceed at lower temperatures even in the presence of 18-crown-6 (Table 2, entry 3–5). Notably, K_2CO_3 did not promote the desired rearrangement, pointing to the importance of the cesium countercation. Radical scavengers did not shut down the reaction as evidenced by the 68% yield obtained when TEMPO was added to the reaction mixture (Table 2, entry 7). Following our initial optimization screen, we discovered that comparable yields of **18** can be obtained over a shorter reaction time of 24 h (Table 2, entry 8).

Computational Details.

In order to shed light on the mechanism of the regioselective ring opening of α-hydroxy-β-lactam **2**, we have undertaken an extensive computational study.

The calculations presented here were carried out using the Gaussian 09 suite of programs.[37] The geometries of all reported reactants, intermediates, transition states (TSs), and products were optimized without symmetry constraints at the B3LYP level of density functional theory (DFT)[38,39] in conjunction with a Lanl2dz basis set and corresponding Hay–Wadt effective core potential (ECP) for Cs and Pd atoms.[40,41] Standard 6-31G(d,p) basis sets were used for all the remaining atoms. Dispersion corrections were included into the calculation at the Grimme's empirical dispersion correction with Becke–Johnson damping for B3LYP.[42] This approach is labeled as [B3LYP-D3Bj]/{Lanl2dz+[6-31G(d,p)]}. Bulk solvent effects are incorporated into calculations at the polarizable continuum model using the integral equation formalism (IEF-PCM) level[43,44] by selecting toluene as the solvent. The nature of each stationary point was characterized by the presence of zero or one imaginary frequency for minima and TS, respectively.

The IRC calculations were performed to confirm the nature of each TS. The relative Gibbs free energies (G) and enthalpies (H) are presented as G/H (in kcal/mol) and calculated under standard conditions (1 atm and 298.15 K), although only the G values are discussed.

Rationalization of Base-Promoted Transition Metal-free Rearrangement.

Given that the Cs_2CO_3-promoted rearrangement was observed as a competing background reaction to the cross-coupling, we initially sought to elucidate the mechanism of this transformation. First, we calculated the distal (C^1—C^2) and proximal (C^α—C^2) bond dissociation free energies (BDFEs) for **2**, which were 45.6 and 39.7 kcal/mol, respectively. For our computational studies, we assume (a) that Cs_2CO_3, rather than derivatives such as $CsHCO_3$ or $CsOH$ (or the corresponding dimeric forms) that may formed in situ, mediates this reaction and (b) a 1:1 (Cs_2CO_3: **2**) binding stoichiometry (see the Supporting Information for full details). In addition, our empirical observation of a dramatic reduction in reaction yield (from 77 to 41% yield) upon changing the solvent from toluene to dioxane

(a more strongly coordinating solvent) indicates the importance of Cs coordination to the substrate. Through our computations, we have identified intermediate **I1** as a prereaction complex (see Figure 6), where one of the Cs cations coordinates to the oxygen of the α-hydroxy group of β-lactam **2** (labeled O^1) and facilitates simultaneous deprotonation of the hydroxy group by CO_3^{2-}.

The calculations reveal that a second Cs cation coordinates (relatively weakly) to the carbonyl oxygen (labeled O^2) of the β-lactam. This latter interaction likely contributes to the observed regioselectivity of the reaction. The calculated free energy of this emerging deprotonation (i.e., lactam + $Cs_2CO_3 \rightarrow$ **I1**) is 33.0 kcal/mol (see Figure 6). We also observe computationally that the deprotonation of **2** by Cs_2CO_3 significantly reduces (by 14–16 kcal/mol) the calculated C—C BDFEs. Specifically, for **I1,** the calculated distal (C^1—C^2) and proximal (C^α—C^2) C—C BDFEs are 31.1 and 23.7 kcal/mol, respectively. The ensuing steps that emerged from intermediate **I1** are a proton transfer from the bicarbonate to C^1 (see **TS1**) and accompanying C^1—C^2 bond weakening. Calculations show that the rotation of the OH bond of the bridging bicarbonate, cleavage of the O^1…HO (bicarbonate) hydrogen bond, and formation of the C^1…H bond initiate the cleavage of the C^1—C^2 bond in **TS1**. The calculated free energy barrier for **TS1** is 28.7 kcal/mol. The close examination of **TS1** shows that it is a late TS, which is consistent with the high (21.3 kcal/mol) endothermicity computed for this reaction. The IRC calculations lead from **TS1** directly to intermediate **I2**. A subsequent proton transfer from bicarbonate to the C^1 center (see **TS2**) is calculated to proceed with only a 1.6 kcal/mol free energy barrier. The overall rearrangement process, which leads to intermediate **I3,** is highly exergonic (by 19.3 kcal/mol). Product release from **I3** requires only 16.9 kcal/mol free energy, which is smaller than the 26.7 kcal/mol free energy required for the reverse reaction. Notably, during the overall transformation, one of the two Cs cations stays coordinated to O^2 through **TS2,** pointing to the critical role of Cs_2CO_3. Its strong coordination to the lactam hydroxy and carbonyl groups significantly reduces the C—C BDFEs, provides a strong base (i.e., carbonate) that facilitates proton transfer from the hydroxy group to C^1, and leads to facile distal C^1—C^2 bond cleavage.

We have also employed the mechanistic insights gained from computation to elucidate the impact of electronic effects on the distal C—C cleavage barriers for **2**. We first studied prereaction complexes and C—C cleavage TSs for a variety of α-hydroxy-β-lactams bearing various para substituents on the aryl ring (see Table 2b). We found that the distal C—C cleavage for **19,** bearing an electron-withdrawing *para*-CF$_3$ group, has a ca 1.9 kcal/mol higher free energy barrier as compared to **2**. In contrast, the barrier for distal C—C cleavage of **20** bearing an electron-donating *para*-OMe group is ca 1.0 kcal/mol lower. Therefore, it appears the electronic density imparted by the aryl ring plays an important role in determining the barrier for C—C cleavage; increased electron density on the aryl ring of the α-hydroxy-β-lactam substrates facilitates the C—C cleavage. This is consistent with our empirical observations. For example, when **19,** which bears an electron-withdrawing group (*para*-CF$_3$), was subjected to the same reaction conditions (Table 2, entry 8), the starting material was predominantly recovered (<18% conversion). However, α-hydroxy-β-lactam **20,** bearing an electron-donating group (4-OMe) on the arene unit, led to full conversion and yielded a 68% yield of the distal cleavage product.

To validate the IEF-PCM approach that we employed, we have calculated structures and relative energies of the $Cs_2CO_3[X]_2$ and $[lactam]Cs_2CO_3[X]_2$ (i.e., **I1**(X)$_2$, see Figure 6) complexes, where X is explicit solvent molecules such as toluene and 1,4-dioxane used in our experiments. We found that solvent molecules only weakly (~3–4 kcal/mol free energies) coordinate to Cs centers. Therefore, we conclude that the inclusion of explicit solvent molecules into our calculations do not significantly impact the results obtained at the [B3LYP-D3BJ]/{Lanl2dz+[6-31G(d,p)]} with the (IEF-PCM) level of theory.[45] Cartesian coordinates and total energies of all reported structures are given in the Supporting Information.

Rationalization of C—C Cleavage/Cross Coupling.

We have also undertaken computational studies to validate the proposed four-step Pd-catalyzed α-arylation of **2** with RuPhos as a ligand (Figure 7). We found two lowest energy isomers, (κ^2-O,O, **I4**) and (κ^2-O,H, **I5**), for the proposed Pd-alcoholate. In the κ^2-O,O isomer (**I4**), the β-lactam moiety is coordinated to the Pd(II) center via the carbonyl and hydroxy oxygens, whereas in the κ^2-O,H isomer (i.e., **I5**), the β-lactam unit and Pd(II) center interact via the hydroxy oxygen and the hydrogen of the C^α—H bond. As one may expect from these coordination motifs, isomer **I4** is 8.0 kcal/mol more favorable as compared to isomer **I5** (see the Supporting Information for more details), which ultimately leads to the α-arylation product. Alcoholates **I4** and **I5** can interconvert through a small energy barrier; therefore, here, we calculate the regioselectivity controlling energy barriers (see **TS3** and **TS4**) relative to the energetically lowest κ^2-O,O isomer (i.e., **I4**). As shown in Figure 7, in **TS3** and **TS4,** the "proximal" and "distal" β-C—C bonds are elongated to 2.01 and 1.98 Å respectively, and the C—O bond is shortened to 1.31 Å in both cases (among other geometry changes). Calculations show that the free energy barrier associated with **TS3,** leading to the α-arylated product, is 0.9 kcal/mol lower than that associated with **TS4,** which is traversed en route to the carbonyl arylation product (i.e., **3a$_d$**). The calculated free energy difference in the regioselective cross-coupling (i.e., 0.9 kcal/mol) is in good agreement with the experimentally observed distribution of these products (9.8:1 of **3a/3a$_d$**; ratio determined by ^{1}H NMR integration using Ph$_3$CH as the internal standard).

Our analysis also reveals that the computed relative lower energy of **TS3** over **TS4** could result from both (a) the weaker C^α—C^2 bond as compared to C^1—C^2 (estimated to be 27.7 and 38.0 kcal/mol, respectively; see the Supporting Information for more details) for the Pd-alcoholate intermediates and (b) a smaller energy requirement for the requisite geometrical deformations in **TS3** as compared to **TS4**. Distortion–interaction[46] calculations have identified the repulsions between the Pd-bound phenyl and isopropyl groups of the RuPhos ligand as major factors that contribute to the geometry distortion of the catalyst in the calculated TSs (see the Supporting Information for details).

CONCLUSIONS

In summary, we report a robust and broadly applicable strategy that achieves the functionalization of piperidines and related saturated nitrogen heterocycles through visible light-mediated lactamization followed by C—C cleavage/cross-coupling protocol. Using an

HTE approach, we identified RuPhos as a uniquely effective ligand for α-arylation and also applied these conditions to achieve alkynylation and vinylation. Moreover, we have identified opportunities for β-arylation of the saturated aza-cycles, which can presumably arise through β-hydride elimination/re-insertion of an α-palladated intermediate. During the course of these studies, a transition metal-free α-acylation was also discovered, demonstrating the unique reactivity of α-hydroxy-β-lactams. Our preliminary studies have identified bases that affect the base-promoted rearrangement (Table 2) and uncovered the role of electronics of the aryl ring of the β-lactam on these processes. On the basis of the proposed mechanistic insights, a more extensive range of ligands will be explored to optimize the distal cleavage/cross-coupling and to identify a general method for β-functionalization. A full account of these studies will be reported in due course.

Supplementary Material

Refer to Web version on PubMed Central for supplementary material.

ACKNOWLEDGMENTS

REFERENCES

(1). Hartwig JF Evolution of C—H Bond Functionalization from Methane to Methodology. J. Am. Chem. Soc 2016, 138, 2–24. [PubMed: 26566092]

(2). Cernak T; Dykstra KD; Tyagarajan S; Vachal P; Krska SW The Medicinal Chemist's Toolbox for Late Stage Functionalization of Drug-Like Molecules. Chem. Soc. Rev 2016, 45, 546–576. [PubMed: 26507237]

(3). Vitaku E; Smith DT; Njardarson JT Analysis of the Structural Diversity, Substitution Patterns, and Frequency of Nitrogen Heterocycles Among U.S. FDA Approved Pharmaceuticals. J. Med. Chem 2014, 57, 10257–10274. [PubMed: 25255204]

(4). Lawrence SA Amines: Synthesis, Properties and Applications; Cambridge University Press: New York, 2004.

(5). For reviews on directing groups in C—H functionalization, see: Sambiagio C; Schönbauer D; Blieck R; Dao-Huy T; Pototschnig G; Schaaf P; Wiesinger T; Zia MF; Wencel-Delord J; Besset T; Maes BUW; Schnürch MA Comprehensive Overview of Directing Groups Applied in Metal-

Catalysed C—H Functionalisation Chemistry. Chem. Soc. Rev 2018, 47, 6603–6743. [PubMed: 30033454] (b)Zhang M; Zhang Y; Jie X; Zhao H; Li G; Su W Recent Advances in Directed C—H Functionalizations using Monodentate Nitrogen-Based Directing Groups. Org. Chem. Front 2014, 1, 843–895.

(6). (a)For selected reviews on a-functionalization of amines, see Mitchell EA; Peschiulli A; Lefevre N; Meerpoel L; Maes BUW Direct a-Functionalization of Saturated Cyclic Amines. Chem.—Eur. J 2012, 18, 10092–10142. [PubMed: 22829434] (b)Campos KR Direct sp3 C—H Bond Activation Adjacent to Nitrogen in Heterocycles. Chem. Soc. Rev 2007, 36, 1069–1084. [PubMed: 17576475]

(7). Coldham I; Leonori D Synthesis of 2-Arylpiperidines by Palladium Couplings of Aryl Bromides with Organozinc Species Derived from Deprotonation ofN-Boc-Piperidine. Org. Lett 2008, 10, 3923–3925. [PubMed: 18683935]

(8). Campos KR; Klapars A; Waldman JH; Dormer PG; Chen C-Y Enantioselective, Palladium-Catalyzed a-Arylation of N-Boc-pyrrolidine. J. Am. Chem. Soc 2006, 128, 3538–3539. [PubMed: 16536525]

(9). Seel S; Thaler T; Takatsu K; Zhang C; Zipse H; Straub BF; Mayer P; Knochel P Highly Diastereoselective Arylations of Substituted Piperidines. J. Am. Chem. Soc 2011, 133, 4774–4777. [PubMed: 21388211]

(10). Millet A; Larini P; Clot E; Baudoin O Ligand-Controlled β-Selective C(sp^3)—H Arylation of N-Boc-Piperidines. Chem. Sci 2013, 4, 2241–2247.

(11). (a)Chen W; Ma L; Paul A; Seidel D Direct a-C—H bond Functionalization of Unprotected Cyclic Amines. Nat. Chem 2018, 10, 165–169. [PubMed: 29359746] (b)Paul A; Seidel D a-Functionalization of Cyclic Secondary Amines: Lewis Acid Promoted Addition of Organometallics to Transient Imines. J. Am. Chem. Soc 2019, 141, 8778–8782. [PubMed: 31117670]

(12). Pastine SJ; Gribkov DV; Sames D Sp^3 C—H bond Arylation Directed by Amidine Protecting Group: a-Arylation of Pyrrolidines and Piperidines. J. Am. Chem. Soc 2006, 128, 14220–14221. [PubMed: 17076471]

(13). (a)Prokopcová H; Bergman SD; Aelvoet K; Smout V; Herrebout W; Van der Veken B; Meerpoel L; Maes BUW C-2 Arylation of Piperidines through Directed Transition-Metal-Catalyzed Sp^3 C—H Activation. Chem.—Eur. J 2010, 16, 13063–13067. [PubMed: 20981669] (b)Peschiulli A; Smout V; Storr TE; Mitchell EA; Eliáš Z; Herrebout W; Berthelot D; Meerpoel L; Maes BUW Ruthenium-Catalyzed a-(Hetero)Arylation of Saturated Cyclic Amines: Reaction Scope and Mechanism. Chem.—Eur. J 2013, 19, 10378–10387. [PubMed: 23780756]

(14). Jain P; Verma P; Xia G; Yu J-Q Enantioselective Amine a-Functionalizations via Palladium-Catalysed C—H Arylation of Thioamides. Nat. Chem 2017, 9, 140–144. [PubMed: 28282045]

(15). Greßies S; Klauck FJR; Kim JH; Daniliuc CG; Glorius F Ligand-Enabled Enantioselective Csp^3—H Activation of Tetrahydro-quinolines and Saturated Aza-Heterocyles by Rh^I. Angew. Chem., Int. Ed 2018, 57, 9950–9954.

(16). Jiang H-J; Zhong X-M; Yu J; Zhang Y; Zhang X; Wu Y-D; Gong L-Z Assembling a Hybrid Pd Catalyst from a Chiral Anionic Co^{III} Complex and Ligand for Asymmetric C(sp^3)—H Functionalization. Angew. Chem., Int. Ed 2019, 58, 1803–1807.

(17). McNally A; Prier CK; MacMillan DWC Discovery of an a-Amino C—H Arylation Reaction using The Strategy of Accelerated Serendipity. Science 2011, 334, 1114–1117. [PubMed: 22116882]

(18). Shaw MH; Shurtleff VW; Terrett JA; Cuthbertson JD; MacMillan DWC Native Functionality in Triple Catalytic Cross-Coupling: Sp^3 C—H Bonds as Latent Nucleophiles. Science 2016, 352, 1304–1308. [PubMed: 27127237]

(19). Beatty JW; Stephenson CRJ Amine Functionalization via Oxidative Photoredox Catalysis: Methodology Development and Complex Molecule Synthesis. Acc. Chem. Res 2015, 48, 1474–1484. [PubMed: 25951291]

(20). Haibach MC; Seidel D C—H Bond Functionalization Through Intramolecular Hydride Transfer. Angew. Chem., Int Ed 2014, 53, 5010–5036.

(21). Davies HML; Hansen T; Hopper DW; Panaro SA Highly Regio-, Diastereo-, and Enantioselective C—H Insertions of Methyl Aryldiazoacetates into Cyclic N-Boc-Protected Amines. Asymmetric synthesis of Novel C2-Symmetric Amines and Threo-Methylphenidate. J.Am. Chem. Soc 1999, 121, 6509–6510.

(22). Rathman TL; Schwindeman JA Preparation, Properties, and Safe Handling of Commercial Organolithiums: Alkyllithiums, Lithium Sec-Organoamides, and Lithium Alkoxides. Org. Process Res. Dev 2014, 18, 1192–1210.

(23). (a)Aoyama H; Hasegawa T; Omote Y Solid state photochemistry of N, N-dialkyl-α-oxoamides. Type II reactions in the Crystalline State. J. Am. Chem. Soc 1979, 101, 5343–5347.(b)For a review on the Norrish–Yang reaction, see: Chen C The Past, Present, and Future of the Yang Reaction. Org. Biomol. Chem 2016, 14, 8641–8647. [PubMed: 27517138]

(24). For a related tandem photochemical/ring-expansion reaction, see: Ishida N; Ne as D; Masuda Y; Murakami M Enantioselective Construction of 3-Hydroxypiperidine Scaffolds by Sequential Action of Light and Rhodium Upon N-Allylglyoxylamides. Angew. Chem., Int. Ed 2015, 54, 7418–7421.

(25). Nishimura T; Uemura S Palladium-Catalyzed Arylation of Tert-Cyclobutanols with Aryl Bromide via C—C Bond Cleavage: New Approach for the γ-Arylated Ketones. J. Am. Chem. Soc 1999, 121, 11010–11011.

(26). Ziadi A; Martin R Ligand-Accelerated Pd-Catalyzed Ketone γ-Arylation via C—C Cleavage with Aryl Chlorides. Org. Lett 2012, 14, 1266–1269. [PubMed: 22332797]

(27). Matsuda T; Matsumoto T; Murakami A Palladium-Catalyzed Ring-Opening Coupling of Cyclobutenols with Aryl Halides. Synlett 2018, 29, 754–758.

(28). Ethirajan M; Oh H-S; Cha JK Formation of Five-Membered Carbocycles by Intramolecular Palladium-Catalyzed Ring Opening of Tert-Cyclobutanols. Org. Lett 2007, 9, 2693–2696. [PubMed: 17579447]

(29). (a)For discussions of precatalysts for cross-coupling, see: Hazari N; Melvin PR; Beromi MM Well-Defined Nickel and Palladium Precatalyst for Cross-Coupling. Nat. Rev. Chem 2017, 1, 0025. [PubMed: 29034333] (b)Shaughnessy KH Development of Palladium Precatalyst that Efficiently Generate LPd(0) Active Species. Isr. J. Chem 2019, 59, 1–16.(c)Bruno NC; Tudge MT; Buchwald SL Design and Preparation of New Palladium Precatalysts for C—C and C—N Cross-Coupling Reactions. Chem. Sci 2013, 4, 916–920. [PubMed: 23667737]

(30). (a)For discussions of $Pd_2(dba)_3$ $CHCl_3$ in catalysis, see: Janusson E; Zijlstra HS; Nguyen PPT; MacGillivray L; Martelino J; McIndoe JS Real-Time Analysis of $Pd_2(dba)_3$ Activation by Phosphine Ligands. Chem. Commun 2017, 53, 854–856.233(b)Zalesskiy SS; Ananikov VP $Pd_2(dba)_3$ as a Precursor of Soluble Metal Complexes and Nanoparticles: Determination of Palladium Active Species for Catalysis and Synthesis. Organometallics 2012, 31, 2302–2309.

(31). For information regarding KitAlysis, see: https://www.sigmaaldrich.com/chemistry/chemical-synthesis/kitalysis-high-throughput-screening-kits.html.

(32). Fu GC The Development of Versatile Methods for Palladium-Catalyzed Coupling Reactions of Aryl Electrophiles through the Use of $P(t-Bu)_3$ and PCy^3 as Ligands. Acc. Chem. Res 2008, 41, 1555–1564. [PubMed: 18947239]

(33). (a)For selected examples of desaturation of amines, see: Bolig AD; Brookhart M Activation of Sp^3 C—H Bonds with Cobalt(I) : Catalytic Synthesis of Enamines. J. Am. Chem. Soc 2007, 129, 14544–14545. [PubMed: 17985901] (b)Bheeter CB; Jin R; Bera JK; Dixneuf PH; Doucet H Palladium-Catalyzed Dehydrogenative Sp^3 C—H Bonds Functionalization into Alkenes: A Direct access to N-Alkenylbenzenesulfonamides. Adv. Synth. Catal 2014, 356, 119–124.(c)Voica A-F; Mendoza A; Gutekunst WR; Fraga JO; Baran PS Guided Desaturation of Unactivated Aliphatics. Nat. Chem 2012, 4, 629–635. [PubMed: 22824894] (d)Chuentragool P; Parasram M; Shi Y; Gevorgyan V General, Mild, and Selective Method for Desaturation of Aliphatic Amines. J. Am. Chem. Soc 2018, 140, 2465–2468. [PubMed: 29400959]

(34). (a)For selected examples of direct remote functionalization of cyclic amines, see: Topczewski JJ; Cabrera PJ; Saper NI; Sanford MS Palldium-Catalysed Transannular C—H Functionalization of Alicyclic Amines. Nature 2016, 531, 220–224. [PubMed: 26886789] (b)Cabrera PJ; Lee M; Sanford MS Second-Generation Palladium Catalyst System for Transannular C—H Functionalization of Azabicycloalkanes. J. Am. Chem. Soc 2018, 140, 5599–5606. [PubMed:

29652497] (c)Steijvoort BFV; Kaval N; Kulago AA; Maes BUW Remote Functionalization: Palladium-Catalyzed C5(Sp^3)-H Arylation of 1-Boc-3-Aminopiperidine through the Use of a Bidentate Directing Group. ACS Catal. 2016, 6, 4486–4490.

(35). MacKinnon AL; Taunton J Target Identification by Diazirine Photo-Cross-Linking and Click Chemistry. Curr. Protoc. Chem. Biol 2009, 1, 55–73. [PubMed: 23667793]

(36). Uehling MR; King RP; Krska SW; Cernak T; Buchwald SL Pharmaceutical Diversification Via Palladium Oxidative Addition Complexes. Science 2019, 363, 405–408. [PubMed: 30679373]

(37). Frisch MJT; Schlegel HB; Scuseria GE; Robb MA; Cheeseman JR; Scalmani G; Barone V; Mennucci B; Petersson GA; Nakatsuji H; Caricato M; Li X; Hratchian HP; Izmaylov AF; Bloino J; Zheng G; Sonnenberg JL; Hada M; Ehara M; Toyota K; Fukuda R; Hasegawa J; Ishida M; Nakajima T; Honda Y; Kitao O; Nakai H; Vreven T; Montgomery JA Jr.; Peralta JE; Ogliaro F; Bearpark M; Heyd JJ; Brothers E; Kudin KN; Staroverov VN; Kobayashi R; Normand J; Raghavachari K; Rendell A; Burant JC; Iyengar SS; Tomasi J; Cossi M; Rega N; Millam MJ; Klene M; Knox JE; Cross JB; Bakken V; Adamo C; Jaramillo J; Gomperts R; Stratmann RE; Yazyev O; Austin AJ ; Cammi R; Pomelli C; Ochterski JW; Martin RL; Morokuma K ; Zakrzewski VG; Voth GA; Salvador P; Dannenberg JJ; Dapprich S; Daniels AD; Farkas Ö; Foresman JB; Ortiz JV; Cioslowski J; Fox DJ Gaussian 09, revision D.01; Gaussian, Inc.: Wallingford CT, 2009.

(38). Becke AD Density-Functional Exchange-Energy Approximation with Correct Asymptotic Behavior. Phys. Rev. A: At., Mol., Opt. Phys 1988, 38, 3098–3100.

(39). Lee C; Yang W; Parr RG Development of the Colle-Salvetti Correlation-Energy Formula into a Functional of the Electron Density. Phys. Rev. B: Condens. Matter Mater. Phys 1988, 37, 785–789.

(40). Hay PJ; Wadt WR Ab Initio Effective Core Potentials for Molecular Calculations. Potentials for the Transition Metal Atoms Sc to Hg. J. Chem. Phys 1985, 82, 270–283.

(41). Wadt WR; Hay PJ Ab Initio Effective Core Potentials for Molecular Calculations. Potentials for Main Group Elements Na to Bi. J. Chem. Phys 1985, 82, 284–298.

(42). Grimme S; Antony J; Ehrlich S; Krieg H A Consistent and Accurate Ab Initio Parametrization of Density Functional Dispersion Correction (DFT-D) for the 94 Elements H-Pu. J. Chem. Phys 2010, 132, 154104. [PubMed: 20423165]

(43). Mennucci B; Tomasi J Continuum Solvation Models: A New Approach to the Problem of Solute's Charge Distribution and Cavity Boundaries. J. Chem. Phys 1997, 106, 5151–5158.

(44). Scalmani G; Frisch MJ Continuous Surface Charge Polarizable Continuum Models of Solvation. I. General Formalism. J. Chem. Phys 2010, 132, 114110. [PubMed: 20331284]

(45). (a)For Recent Examples of DFT-Supported Mechanisms Involving Cs Cations, see: Li B-W; Wang M-Y; Fang S; Liu J-Y DFT Study on the Mechanism of Palladium(0)-Catalyzed Reaction of Aryl Iodides, Norbornene, and Di-tert-butyldiaziridinone. Organometallics 2019, 38, 2189–2198.(b)Xu H; Muto K; Yamaguchi J; Zhao C; Itami K; Musaev DG Key Mechanistic Features of Ni-Catalyzed C─H/C─O Biaryl Coupling of Azoles and Naphthalen-2-yl Pivalates. J. Am. Chem. Soc 2014, 136, 14834–14844. [PubMed: 25259782]

(46). Ess DH; Houk KN Distortion/Interaction Energy Control of 1,3-Dipolar Cycloaddition Reactivity. J. Am. Chem. Soc 2007, 129, 10646–10647. [PubMed: 17685614]
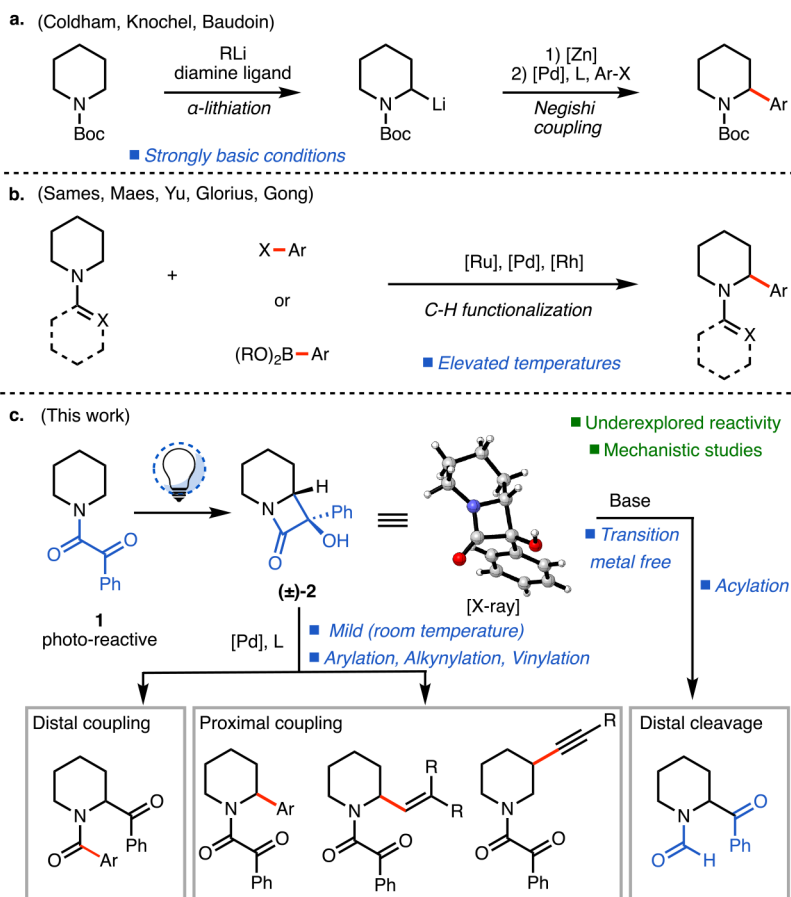
Figure 1.
Approaches to α-functionalization of piperidines by C—H functionalization. (a) Reported α-functionalization utilizing the lithiation/Negishi cross-coupling sequence. (b) Selected examples of C—H functionalization approaches for piperidine α-functionalization. (c) Strain release approach for mild cyclic amine functionalization (this work).
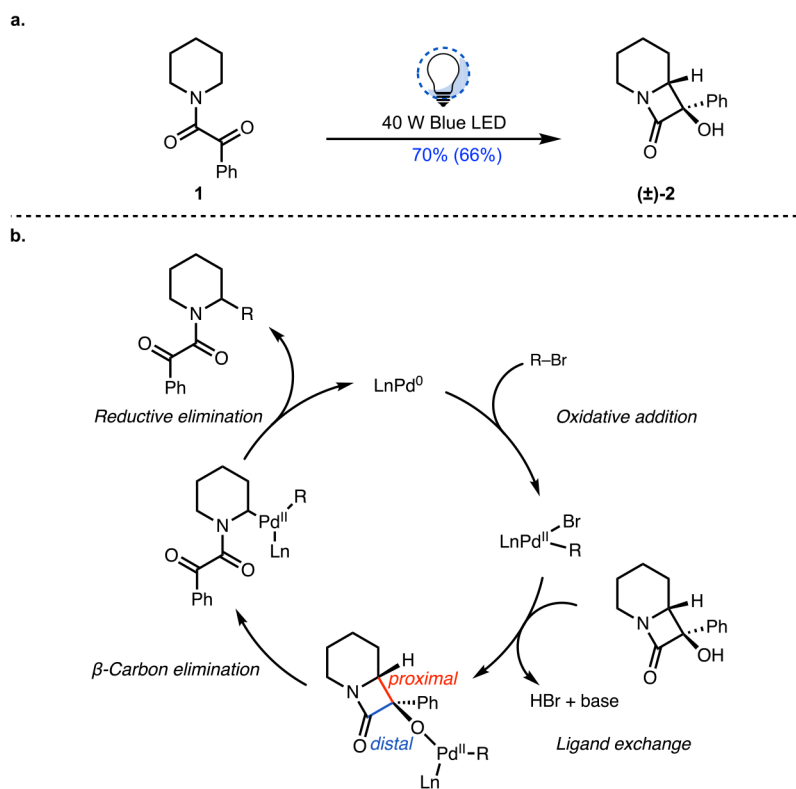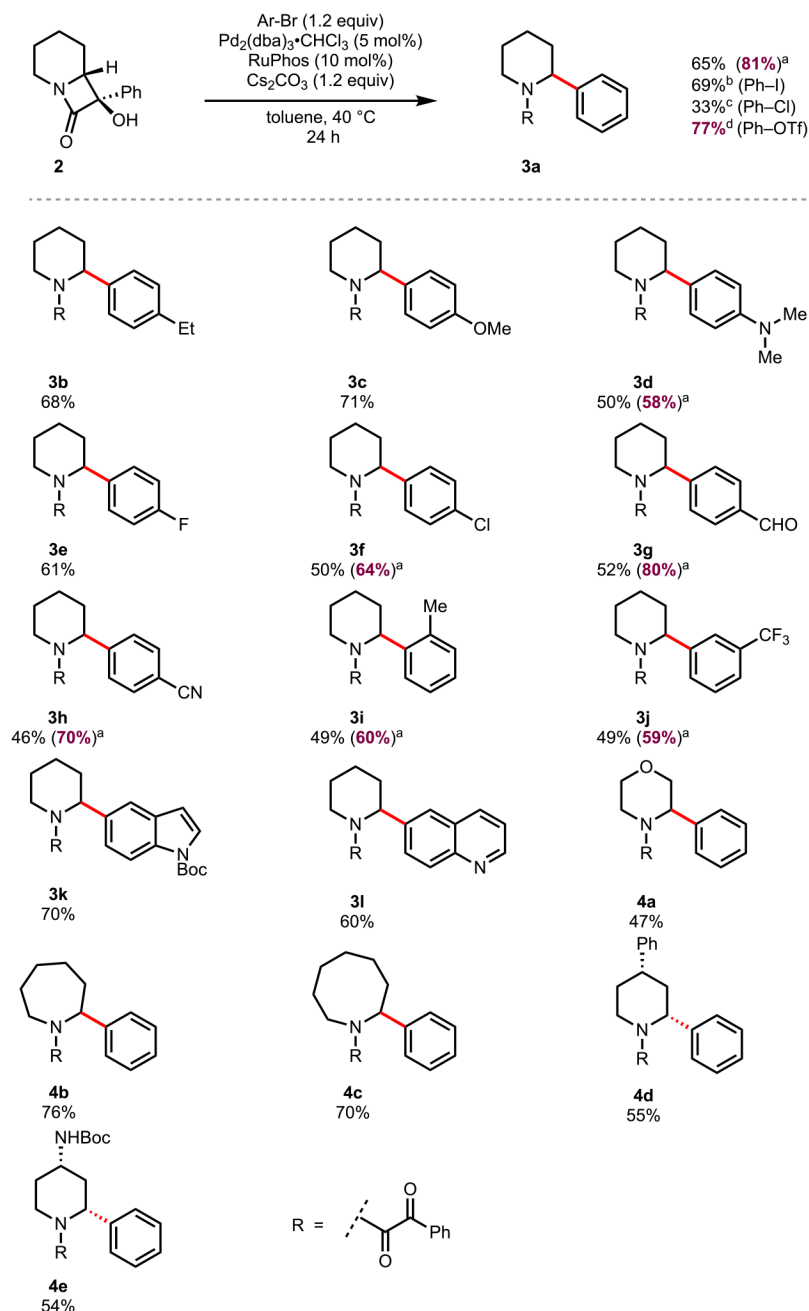
Figure 2.
Reaction design. (a) Norrish–Yang protocol. Yield was determined by ^{1}H NMR integration using Ph$_3$CH as the internal standard. Isolated yield is shown in parentheses. (b) Proposed catalytic cycle.

Figure 3.
Scope of the arylation reaction. All yields reported are isolated yields, unless otherwise stated. Reactions were performed with **2** (0.10 mmol), Ar—Br (0.12 mmol), $Pd_2(dba)_3 \cdot CHCl_3$ (5 mol %), RuPhos (10 mol %), Cs_2CO_3 (0.12 mmol), and toluene (0.2 M) at 40 °C for 24–48 h. (a) Reactions were performed with **2** (0.10 mmol), Ar—Br (0.12 mmol), RuPhos-Pd-G4 (10 mol %), Cs_2CO_3 (0.20 mmol), and toluene (0.2 M) at 40 °C for 24–48 h. (b) Ph—I (0.12 mmol) was used instead of Ph—Br. (c) **2** (0.10 mmol), Ph—Cl (0.12 mmol), $Pd_2(dba)_3 \cdot CHCl_3$ (5 mol %), XPhos (10 mol %), Cs_2CO_3 (0.12 mmol), and toluene (0.2 M) at 100 °C for 24 h. Yields were determined by ^{1}H NMR integration using

Ph$_3$CH as the internal standard. (d) Reactions were performed with **2** (0.10 mmol), Ar—OTf (0.12 mmol), RuPhos-Pd-G4 (10 mol %), Cs$_2$CO$_3$ (0.20 mmol), and toluene (0.2 M) at 40 °C for 24 h. See the Supporting Information for detailed conditions of each substrate.
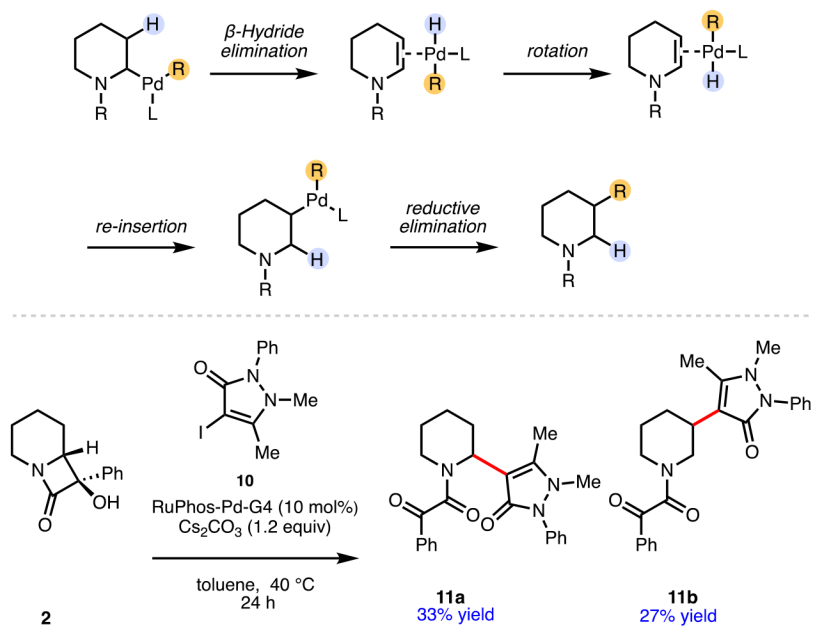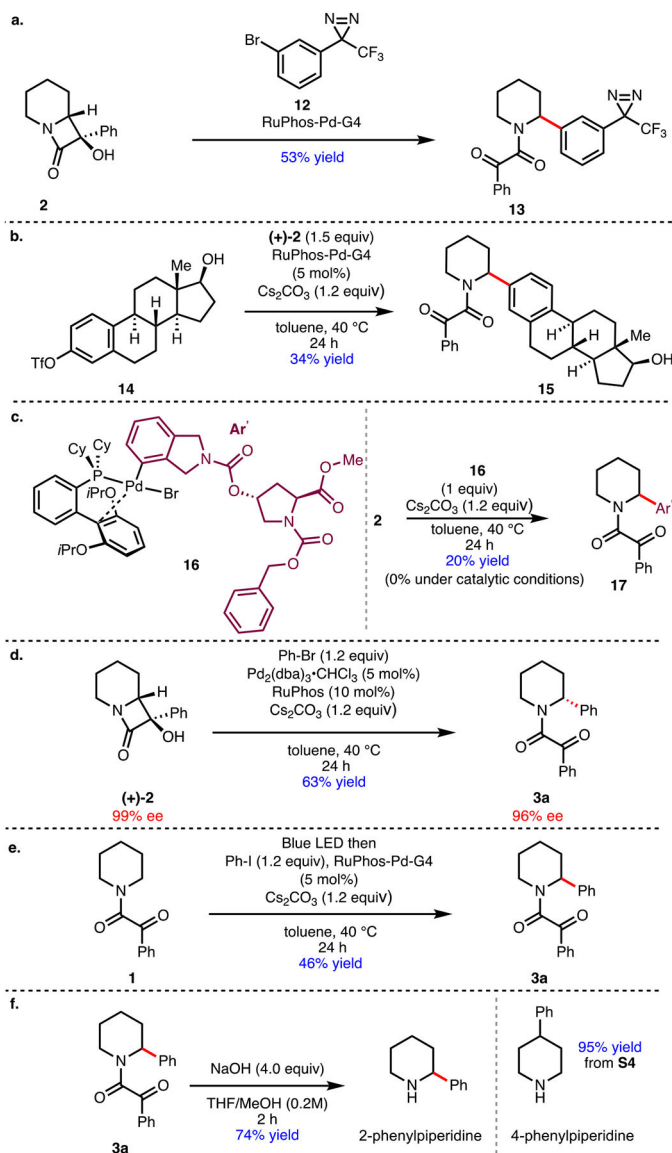
Figure 4.
Substrate-controlled selectivity.

Figure 5.
Broad-ranging scope for functionalization. See the Supporting Information for detailed experimental conditions. (a) Mild coupling conditions tolerate a trifluoromethyldiazirine functional group. (b) LSF. (c) Pd(II) oxidative addition complexes can serve as coupling partners. (d) Cross-coupling with the enantioenriched material supports a highly stereoretentive process. (e) One-pot arylation. (f) Removal of the keto amide group.
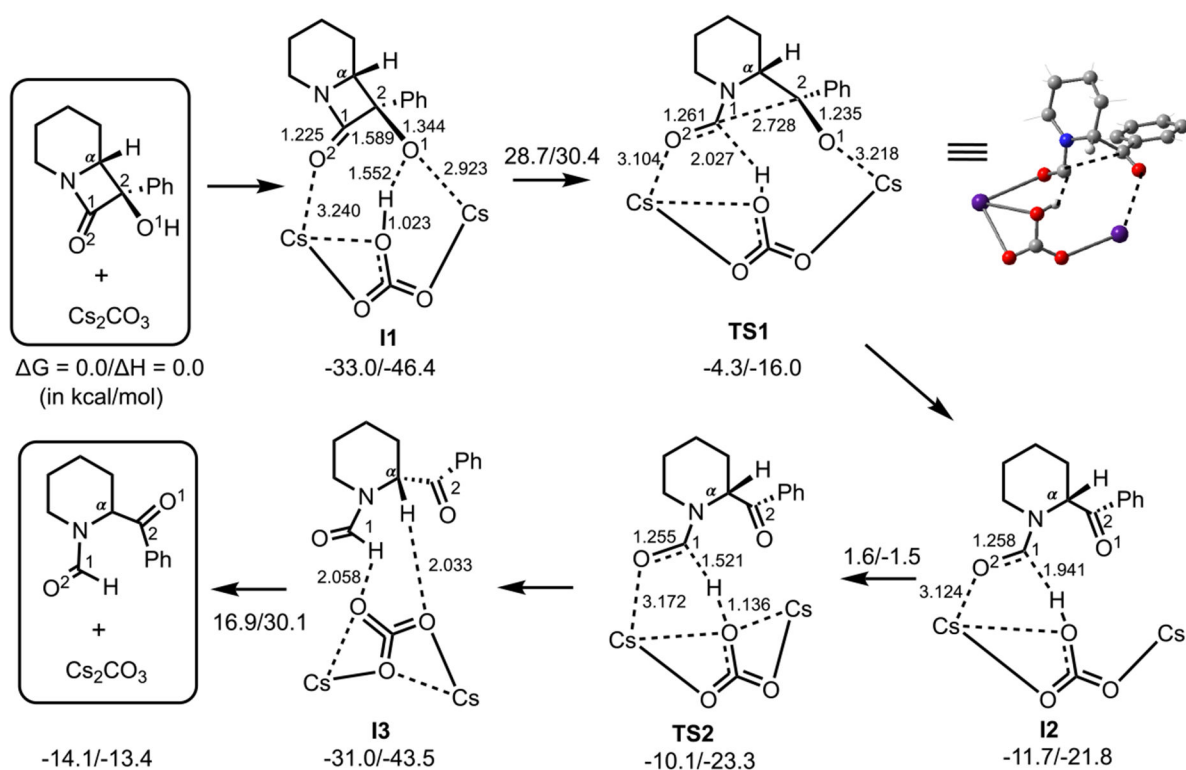
Figure 6.

Schematic representation of the calculated reactant, intermediates, TSs, and product for the "distal" C^1—C^2 bond cleavage of α-hydroxy-β-lactam **2** in the presence of Cs_2CO_3. Bond distances are in Å.
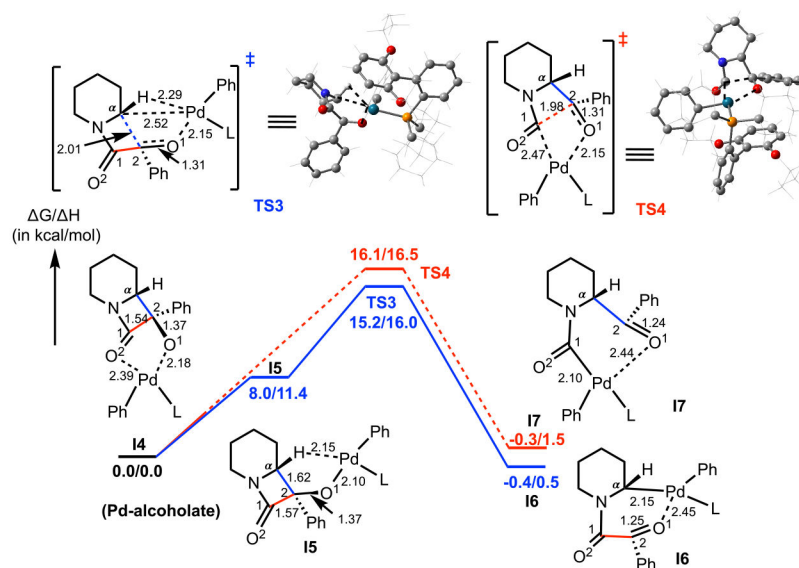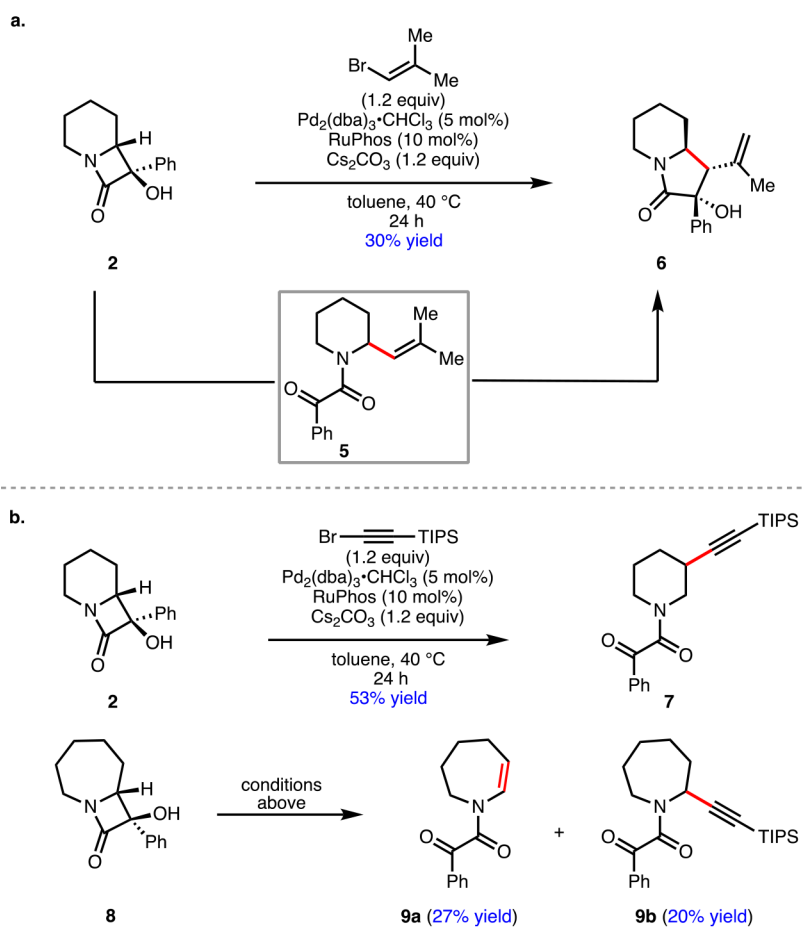
Figure 7.
Schematic representation of the free energy surfaces (energies are in kcal/mol), calculated Pd-alcoholate intermediates, regioselectivity-determining TSs, and products of the "proximal" β-C^α—C^2 and "distal" β-C^1—C^2 bond cleavage step of α-hydroxy-β-lactam **2**. Bond distances are in Å. (see the Supporting Information for full details).

a.

b.

Scheme 1. Development of α-Vinylation and α/β-Alkynylation[a]

[a]Reactions were performed with lactam (0.10 mmol), 1-bromo-2-methylprop-1-ene (0.12 mmol) (0.12 mmol), Pd$_2$(dba)$_3$·CHCl$_3$ (5 mol %), RuPhos (10 mol %), Cs$_2$CO$_3$ (0.12 mmol), and toluene (0.2 M) at 40 °C for 24–48 h. For alkynylation, (bromoethynyl)triisopropylsilane (0.12 mmol) was used instead of 1-bromo-2-methylprop-1-ene (0.12 mmol).

Table 1.

Reaction Development; Optimization of α-Arylation Reaction
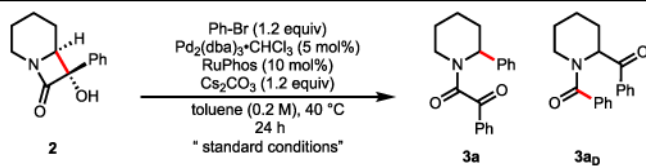
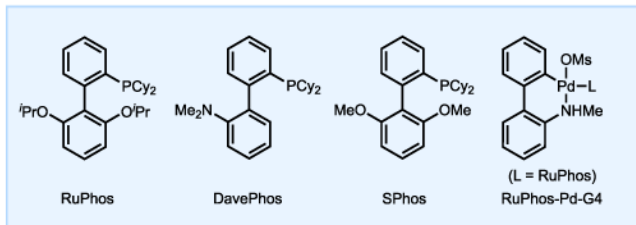| entry	deviations from the standard conditions	yield
1	none	65%(**3a**), 6%(**3a_D**)
2	DavePhos instead of Ruphos	42%(**3a**), 8%(**3a_D**)
3	SPhos instead of Ruphos	22%(**3a**), 10%(**3a_D**)
4	K₃PO₄ instead of Cs₂CO₃	37% (**3a**)
5	K₂CO₃ instead of Cs₂CO₃	16% (**3a**)
6	1,4-dioxane instead of toluene	0%
7	room temperature	7% (**3a**)
8	Ruphos-Pd-G4 (10 mol%), Cs₂CO₃ (2.0 equiv), rt	66% (**3a**)
9	Ruphos-Pd-G4 (10 mol%), Cs₂CO₃ (2.0 equiv), rt 40 °C	81% (**3a**)

Table 2.

Discovery of a Base-Promoted Rearrangement; (a) Optimization of Reaction Conditions; (b) Influence of the Aryl Substituent on Base-Promoted Reaction

entry	deviations from the standard conditions	yield
1	none	77%
2	1,4-dioxane instead of toluene	41%
3	40 °c instead of 60 °C	0%
4	rt instead of 60 °C	0%
5	40 °C instead of 60 °C, 18-crown-6 (1.5 equiv)	0%
6	K₂CO₃ instead of Cs₂CO₃	0%
7	TEMPO (2.0 equiv) added	68%
8	24 instead of 48h	78%